Comparative Switching and Conduction Loss Analysis of a SVPWM and DPWM based DTC of Open-End Winding Induction Motor Drive

Siliveru Sarada *, Dr.N.Ravisankara Reddy **‡

*Department of EEE, Research Scholar, JNTUA, Anantapuramu.

**Department of EEE, Associate Professor, G.Pulla Reddy Engineering College, Kurnool

(saradasasi@gmail.com, netapallyravi@gmail.com)

‡Corresponding Author; Siliveru Sarada, Department of EEE, Research Scholar, JNTUA, Anantapuramu,

Tel: +918498969629, saradasasi@gmail.com

Received: 20.09.2022 Accepted:21.10.2022

Abstract- Multi Level Inverter (MLI) fed Direct Torque Control (DTC) exhibit superior dynamic performance. MLIs offers low stress on switching devices and allow devices with low voltage rating against high dc link voltage for a medium and high voltage drives. Dual inverter based MLI topology has gained popularity as each inverter operated as a two-level inverter. An improvised loss analysis is carried out for a DTC control based three level dual inverter fed Open End Winding Induction Motor (OEWIM) drive is implemented in this paper. Switching and conduction losses are the measure of conversion efficiency of an inverter. These losses are also causing high junction temperature and consequent device failure. Higher the switching and conduction losses lower will be the conversion efficiency. So, it is necessary to quantify these losses for the safe operation of the switching devices is concerned. These losses are depending mainly on type of Pulse Width Modulation (PWM) scheme used for the generation of pulse pattern. Comparative loss analysis as a function of modulation index for Decoupled and Alternate Inverter Switching (AIS) based Space Vector PWM (SVPWM) and Discontinuous PWM (DPWM) schemes. So based on the operating conditions, a particular PWM scheme can be selected.

Keywords DTC, SVPWM, DPWM, Switching and Conduction Losses.

1. Introduction

Most of the industrial applications require variable speed drives in order to obtain saving in energy. In classical days, induction motors are employed in constant speed drives only because, power semiconductor devices available on those days at the early stage of development. After invent of IGBT (Insulated Gate Bipolar Transistor), the drives technology has been stepped into new era. As the semiconductor device technology progresses, parallel development has been occurred in induction motor drives. Now a days, induction motor drives extensively used in variable speed applications owing to IGBT based Voltage Source Inverter (VSI)s. Added to this, induction motors are rigid in construction, easy adoption into various types of industrial loads.

The variable speed drives can be realized either by scalar control or vector control schemes. Volts/Hz control falls under the category of scalar control. In which voltage magnitude is changed based on the operating frequency. The main disadvantage of scalar control scheme is that poor dynamic response, sensitive to parameter variation etc. These disadvantages can be overcome in vector control scheme, in which magnitude as well as angle of the voltage vector is taken into account. In vector control there are two variants such as, Field Oriented Control (FOC) and Direct Torque Control (DTC). FOC is difficult to implement as it involves coordinated transformation and other complex mathematical manipulations. DTC scheme was developed in [1] is the most widely used control scheme as it offers fast dynamic response. But classical DTC suffers from high torque and flux ripple, as it employs hysteresis controllers in torque and

flux loop. Nevertheless, operation involves variable frequency as a result, filter design becomes tedious. Torque and flux ripples are minimized by Multi Level Inverters (MLI) and Space Vector Modulation (SVM) [2]-[4] scheme offers constant switching frequency.

Among various MLI topologies, Open End Winding Induction Motor (OEWIM) [5] topology became popular. Space Vector Pulse Width Modulation (SVPWM) is one of the most widely used PWM scheme, as it enables better dc bus utilization and low harmonic distortion [6].

Switching loss and conduction loss are the measure of conversion efficiency of an inverter. Higher the switching loss lower will be the conversion efficiency. Switching losses are more in case of SVPWM as the switching devices in VSI will operate continuously over the fundamental cycle. In order to counteract higher switching losses, Discontinuous Pulse Width Modulation (DPWM) [7] techniques were introduced. In which, switching devices are clamped to dc bus over certain interval of time and rest of the interval, the devices are going to operate in ON and OFF fashion. Hence switching losses are less in case of DPWM as compared to SVPWM.

MLIs are found in medium and high voltage applications. These converters have high power handling capability and also produce high voltage best in class waveform quality. An IGBT based MLIs operating at high switching frequency reduce the harmonic content in output voltage. So in order to reduce the size of the filtering components, switching frequency should be increase and therefore switching losses increases thereby reducing the system efficiency. Since there are many number of switching devices in MLIs, switching loss problem becomes more serious. So, it is necessary to quantify the switching losses of the MLI.

The major problems associated with MLIs are that the power loss in an IGBT results in increase in the junction temperature, distort its characteristics and reduces its lifespan. The increase in junction temperature of the switching device can be addressed by quantifying the total switching power loss, which depends not only on the switching frequency, on-state resistance of the switching device [8], but also on the PWM scheme used for inverter. The semiconductor losses in VSI are divided into static loss and non-static loss [9]. Among them conduction and switching losses are the major losses. The blocking and driving losses are usually not significant.

The work presented in [10] and [11] was the thermal analysis for three-level Open End Winding Induction Motor Drive (OEWIMD) with the help of a loss model. In which conduction and switching losses of the IGBT was taken into account only. But conduction loss of the anti-parallel diode was not taken into account. In this paper, the switching loss and conduction loss were evaluated for the dual inverter driven Decoupled and Alternate Inverter Switching (AIS) based Space Vector PWM (SVPWM) based 3-level OEWIMD presented in [11]. Also, an improved loss model was developed in [12] used to quantify the losses associated with Decoupled and AIS based Discontinuous Pulse Width Modulation (DPWM) schemes for the 3-level OEWIM with a greater accuracy. [14]-[21] investigated loss minimization PWM schemes proposed for Neutral Point Clamped (NPC), T-type Neutral Point Clamped (TNPC) and Cascaded H-Bridge (CHB) inverters. However, these MLIs has limitations such as neutral point voltage balancing in NPC and large no. of sources required in CHB inverters. Ripple current reduction [22] for DTC of DFIG and [23]-[27] calculated the switching losses as a function of power factor angle of the load based on vector approach [24]-[27] and carrier approach [23] for two-level voltage source inverter and for Modular Multi Level Inverter [28]. Switching devices in two-level inverters subjected to large voltage stress in high power applications causing switching losses to rise. [29] proposed dodecagonal space vector modulation to reduce switching loss and lower order harmonics for a dual inverter fed induction motor drive. [29] reported a control scheme for Z-Source Inverter (ZSI), in which Switching losses, conduction losses and total power loss were calculated for ZSI as a function of switching frequency based on vector approach, which involves determination of location of reference voltage vector [28]-[29].

The loss model used in this paper not only accounted for the conduction loss occurs in the anti-parallel diodes, but also loss due to reverse recovery phenomenon. The total loss occurred in total drive system is the sum of i) IGBT's switching and conduction power loss ii) anti-parallel diode's conduction loss iii) power loss occurs due to reverse recovery phenomenon in body diode. The comparative analysis of 3-level inverter fed OEWIMD is carried out in terms of total dual inverter losses for Decoupled and AIS based SVPWM and DPWM schemes.

2. Dual Inverter Topology

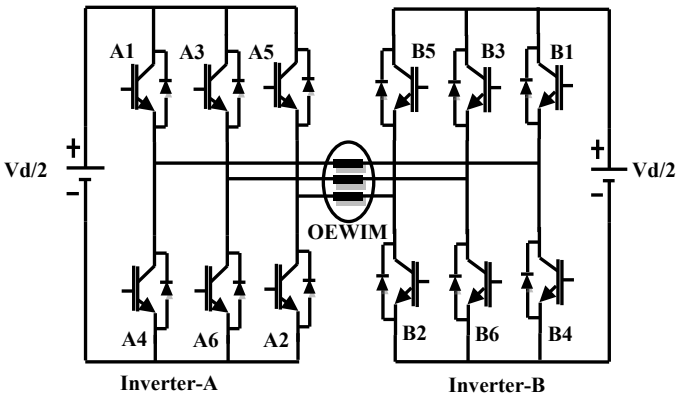

Fig.1. Three Level dual inverter fed open end winding induction motor.

Fig.1 shows the power circuit diagram of dual inverter fed OEWIM drive. Two isolated dc voltage sources each of magnitude Vd/2 is applied to each of the inverter's A & B to generate 3-level voltage waveform. With the help of PWM schemes, the detailed operation of Dual Inverter was explained in section-4. Pole voltages of the inverter-A are $(Voa)_A$, $(Vob)_A$ and $(Voc)_A$ and pole voltages of inverter-B are $(Voa)_B$, $(Vob)_B$ and $(Voc)_B$ and effective pole voltages are (Voa), (Vob) and (Voc) . The effective pole voltage of a,b, and c phases are determined by (1) as follows

$$(V_{oi}) = (V_{oi})_A - (V_{oi})_B \qquad (1)$$

where $i = a, b, c$

3. Direct Torque Control

Fig.2 shows the block diagram of a DTC of Open-End Winding induction motor drive.

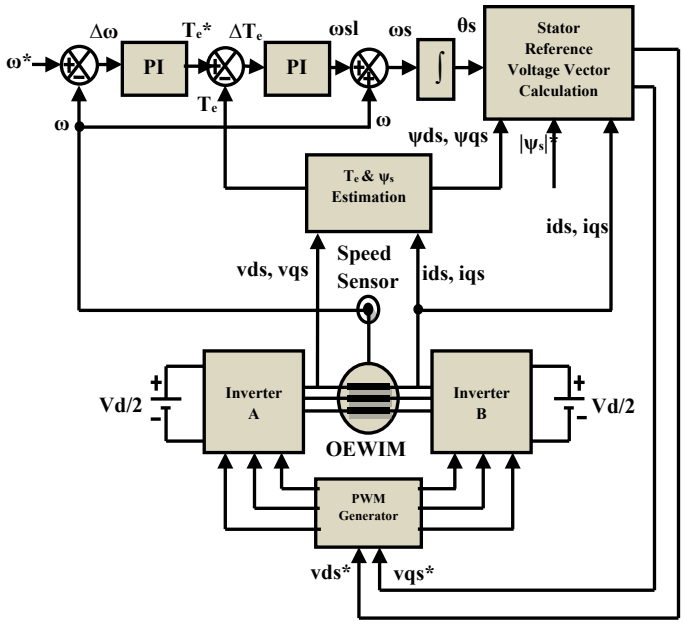

Fig.2. Block Diagram of a DTC of Open-End Winding induction motor drive.

The electromagnetic torque developed by the 3-Φ induction motor can be written as

$$T_e = \frac{3}{2}\frac{P}{L_s^1}\frac{L_m}{L_r}\left|\psi_s\right|\left|\psi_r\right|\sin\delta \qquad (2)$$

It can be seen that from above equation, electromagnetic torque developed by the motor is function of the stator flux, rotor flux and the phase angle between stator flux and rotor flux. The torque of the motor can be varied by varying the either stator flux magnitude or rotor flux magnitude or angle between them. As the time constant of the rotor circuit is more than the stator circuit, control of the rotor flux leads to poor dynamic response of the drive. Hence by keeping the rotor flux constant, variation of stator flux can be controlled to track reference torque. In stationary reference frame, stator voltage equation can be expressed as

$$\bar{V}_S = \bar{I}_S R_S + \frac{d\bar{\psi}_S}{dt} \qquad (3)$$

In infinitesimal time interval, the resistance of the stator can be neglected (except at low-speed operation). By applying appropriate voltage vector, stator flux can be changed and hence change in phase angle between two fluxes and therefore torque is controlled. This can be expressed mathematically as

$$\Delta\bar{\psi}_S = \bar{V}_S \Delta t \qquad (4)$$

The error in corresponding d-axis and q-axis fluxes can be calculated as follows.

$$\Delta\bar{\psi}_{ds} = \bar{\psi}^*_{ds} - \bar{\psi}_{ds} \qquad (5)$$

$$\Delta\bar{\psi}_{qs} = \bar{\psi}^*_{qs} - \bar{\psi}_{qs} \qquad (6)$$

With the knowledge of resistance of the stator and error in fluxes over interval Ts can be used to find the d-axis and q-axis commanded voltages as follows.

$$V_{ds}^{\ *} = I_{ds}R_S + \frac{\Delta\psi_{ds}}{T_S} \qquad (7)$$

$$V_{qs}^{\ *} = I_{qs}R_S + \frac{\Delta\psi_{qs}}{T_S} \qquad (8)$$

The d-axis and q-axis commanded voltages can be used to generate the modulating by addition of zero sequence signal and sinusoidal reference signal explained as under.

4. Pulse Width Modulation Schemes

SVPWM offers lower harmonic distortion and better DC bus utilization. SVPWM falls under the category of Continuous Pulse Width Modulation (CPWM) scheme as the modulating signal is continuous. However, the major limitation of SVPWM scheme is subjected to high switching losses as the devices in inverter operate in the manner ON and OFF continuously over the entire fundamental cycle. In DPWM schemes, the switching losses are low about 1/3rd compared to SVPWM scheme as the switching devices are clamped to dc bus over certain interval of time and rest of the interval, the devices are going to operate at carrier frequency.

To implement SVPWM and DPWM schemes either space vector or carrier based scalar approach can be used. Both these approaches give identical results by selecting the appropriate modulating signal. However, knowledge of reference voltage vector location and complex mathematical manipulations space vector approach becomes cumbersome. In order to handle this problem, modulating signal can be generated either addition of zero sequence signal with the sinusoidal reference signal or method of imaginary switching times. In this paper, addition of zero sequence signal to the reference signal approach was implemented.

Let the reference signals for three phases are

$$Vix = V_m\cos(\omega t - 2(k-1)\frac{\pi}{3}) \qquad (9)$$

$$Viy = V_m\cos(\omega t - 2(k-1)\frac{\pi}{3} - \frac{\pi}{6}) \qquad (10)$$

Where i = a, b, c and k =1, 2, 3

The zero sequence and modulating signal are expressed mathematically as under.

$$V_Z = \frac{Vd}{2}(2a_o - 1) - a_o V_{\max} + (a_o - 1)V_{\min} \quad (11)$$

where Vmax = max (Vi) and Vmin = min (Vi)

$$V_i^* = V_i + V_Z \quad (12)$$

By proper selection of a_o and V_i different modulation signals can be synthesized as given in table.1. As the no. of output voltage levels increased, space vector scheme was difficult to implement and therefore carrier-based approach was implemented in this paper. In this approach, switching spectrum was generated by comparing high frequency carrier (triangular) signal and modulating signals as shown in Fig.3 and Fig.4.

Table 1. Generation of Modulating Signal as a function of ao

S.No.	Mod. Scheme	Ref. Signal	Condition	a_o
1	SVPWM	Vix	---	0.5
2	DPWM MIN	Vix	---	0
3	DPWM MAX	Vix	---	1
4	DPWM0	Viy	$V_{\max} + V_{\min} < 0$	1
			$V_{\max} + V_{\min} \geq 0$	0
5	DPWM1	Vix	$V_{\max} + V_{\min} < 0$	0
			$V_{\max} + V_{\min} \geq 0$	1
6	DPWM2	Viy	$V_{\max} + V_{\min} < 0$	0
			$V_{\max} + V_{\min} \geq 0$	1
7	DPWM3	Vix	$V_{\max} + V_{\min} < 0$	1
			$V_{\max} + V_{\min} \geq 0$	0

The switching logic for generation of firing pulses for Decoupled PWM and AIS PWM schemes is given in Table 2. and Table 3 respectively. In case of Decoupled PWM scheme, both inverters viz. Inverter-A and Inverter-B are operated simultaneously, whereas in case of AIS PWM, while Inverter-A is operating, Inverter-B is clamped to 0V and vice-versa i.e inverters are operating alternately for every 180^O. In case of Decoupled PWM, two reference signals V_{r1} and V_{r2} compared with carrier signal Vc to generate pulse pattern. In which, V_{r1} is used to generate pulse pattern for inverter-A and V_{r2} is used to generate pulse pattern for inverter-B.

In case of AIS PWM, one reference signal V_r is compared with two level shifted carrier signals V_{c1} and V_{c2}. In which, V_{c1} is used to generate pulse pattern for inverter-A and V_{c2} is used to generate pulse pattern for inverter-B. The nomenclature used in Table 2 and Table 3 for switching action is depicted as follows; ON (switch remains continuously in ON condition over 180^O), OFF (switch remains continuously in OFF condition over 180^O) and Operating (Op.) means switch operates at carrier frequency (both ON and OFF).

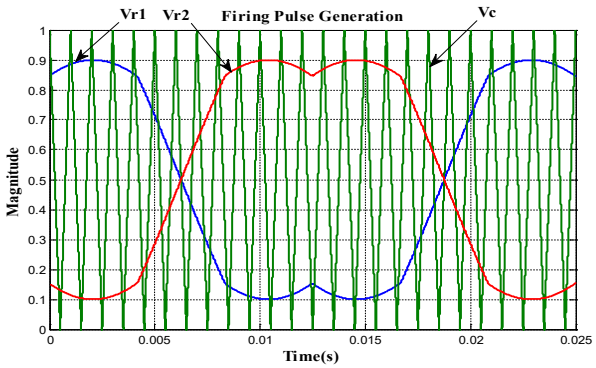

Fig. 3. Carrier Based Approach in Decoupled PWM for Firing Pulse Generation.

Table 2. Switching Logic for Generation of Firing Pulses for Decoupled PWM

S. No	Condition	Status of Inverters Switches				Pole Voltage of Inv-A	Pole Voltage of Inv-B	Effective Pole Voltage
		A1	B1	A4	B4			
1.	$V_{r1} > V_c$	ON	---	OFF	---	Clamped to Vd/2	---	Voltage levels between Vd/2 & 0
2.	$V_{r1} < V_c$	OFF	---	ON	---	Clamped to 0V	---	
3.	$V_{r2} > V_c$	---	OFF	---	ON	---	Clamped to 0V	Voltage levels between 0 & -Vd/2
4.	$V_{r2} < V_c$	---	ON	---	OFF	---	Clamped to Vd/2	

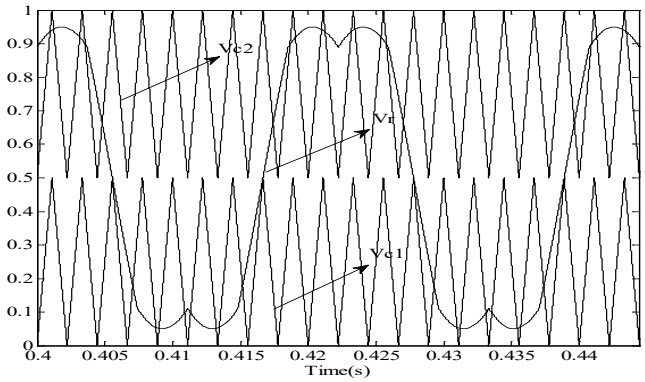

Fig.4. Carrier Based Approach in AIS PWM Strategy for Firing Pulse Generation.

Table 3. Switching Logic for Generation of Firing Pulses for AIS PWM

S. No	Condition	Status of Inverters Switches				Pole Voltage of Inv-A	Pole Voltage of Inv-B	Effective Pole Voltage
		A1	B1	A4	B4			
1.	$V_r \geq V_{c1}$	ON	---	OFF	---	Clamped to 0V	Operating between Vd/2 & 0	Voltage levels between 0 & Vd/2
2.	$V_r < V_{c1}$	Op.	---	Op.	---	Operating between Vd/2 & 0	Clamped to 0V	
3.	$V_r < V_{c2}$	---	ON	---	OFF	Operating between Vd/2 & 0	Clamped to 0V	Voltage levels between 0 & -Vd/2
4.	$V_r \geq V_{c2}$	---	Op.	---	Op.	Clamped to 0V	Operating between Vd/2 & 0	

In case of AIS PWM, one reference signal is compared with two level shifted carrier signals Vc1 and Vc2. In which, Vc1 is used to generate pulse pattern for inverter-A and Vc2 is used to generate pulse pattern for inverter-B. The nomenclature used in table.2 and table.3 for switching action is depicted as follows; ON (switch remains continuously in ON condition over 180^O), OFF (switch remains continuously in OFF condition over 180^O) and Op. (Operating) switch operates at carrier frequency (both ON and OFF).

5. Switching and Conduction Loss Analysis of PWM Schemes

The loss analysis of Decoupled and AIS based SVPWM and DPWM schemes for the three-level inverter fed OEWIMD is carried out here. One leg of a phase-a of the dual inverter is shown in Fig.5. It comprises of two IGBT devices (A1, A4) and their anti-parallel diodes (D1, D4) respectively. The current through and voltage across and the top device and its anti-parallel diode connected to the bottom switch including the diode reverse recovery current are also shown in Fig.5.

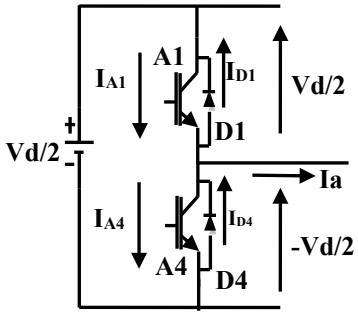

Fig.5. One leg of a Phase-a of Inverter-A.

The expression for switching power loss (P_{sw}) and conduction loss (P_{Cond}) is given by [8]

$$P_{sw} = \left[\frac{1}{2} v_{sw} i_{sw} (t_{ri} + t_{fv}) + \frac{1}{2} v_{sw} i_{sw} (t_{rv} + t_{fi})\right] f_{sw} \quad (13)$$

$$P_{cond} = \frac{V_{on} I_{on} t_{on}}{T_s} \quad (14)$$

where,

v_{sw} = Blocking voltage of the switch (i.e. Vd /2),

i_{sw} = Ion = Instantaneous rated phase current,

f_s = Switching frequency,

$T_s = 1/f_s$ = Switching time period,

V_{on} = On state voltage drop of switch,

t_{ri} = Rise time of the current,

t_{fi} = Fall time of the current,

t_{rv} = Rise time of the voltage,

t_{fv} = Fall time of the voltage,

ton = Switch ON time.

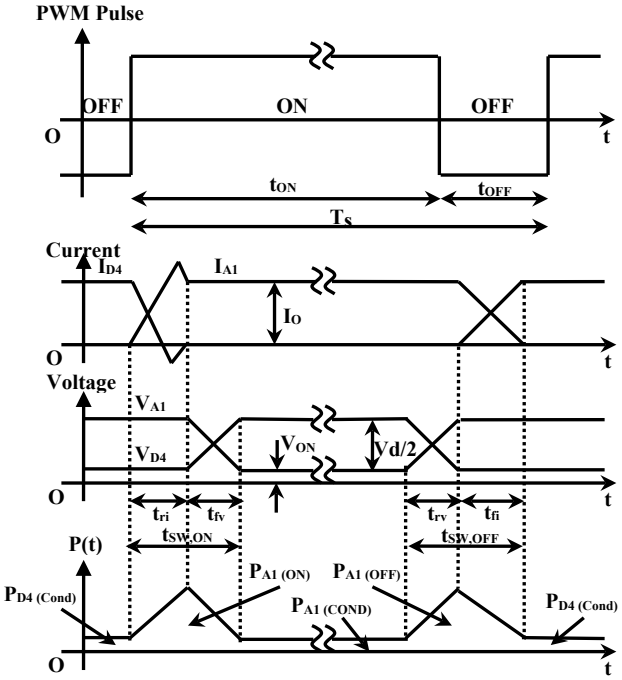

Fig.6. Voltage across and current through the top switch (A1) and bottom diode (D4) [8]

The switching and conduction losses of the three-level inverter fed OEWIM drive were calculated using the loss-model proposed in [11]. But, the loss-model proposed in [11] assumes that the anti-parallel diodes were ideal devices, conduction loss and the loss due to the reverse recovery phenomenon in them were neglected. In [13], the losses were calculated with the help of an improvised loss-model, which includes power loss due to the practical anti-parallel diodes and reverse recovery phenomenon in them. Total dual inverter losses are the sum of switching and conduction losses.

6. Results and Discussion

Fig.7 shows modulating signals for SVPWM, DPWMMIN, DPWMMAX, DPWM0, DPWM1, DPWM2 and DPWM3. These modulating signals are compared with carrier signals to generate switching spectrum for the operation of switching devices as explained in section-4. Among these, SVPWM scheme generate continuous modulating signal and hence termed as continuous PWM, whereas rest of the PWM schemes generate discontinuous modulating signal and hence termed as discontinuous PWM schemes. In case of continuous PWM scheme, the switch is operating at carrier frequency continuously over the fundamental cycle, whereas in case of discontinuous modulating scheme, the switch is either clamped to maximum dc bus voltage or clamped to 0 volts over certain interval of time, rest of the interval the switch is operate at carrier frequency depending upon the various types of DPWM schemes. Therefore, switching losses are found to be less for DPWM schemes compared with SVPWM scheme.

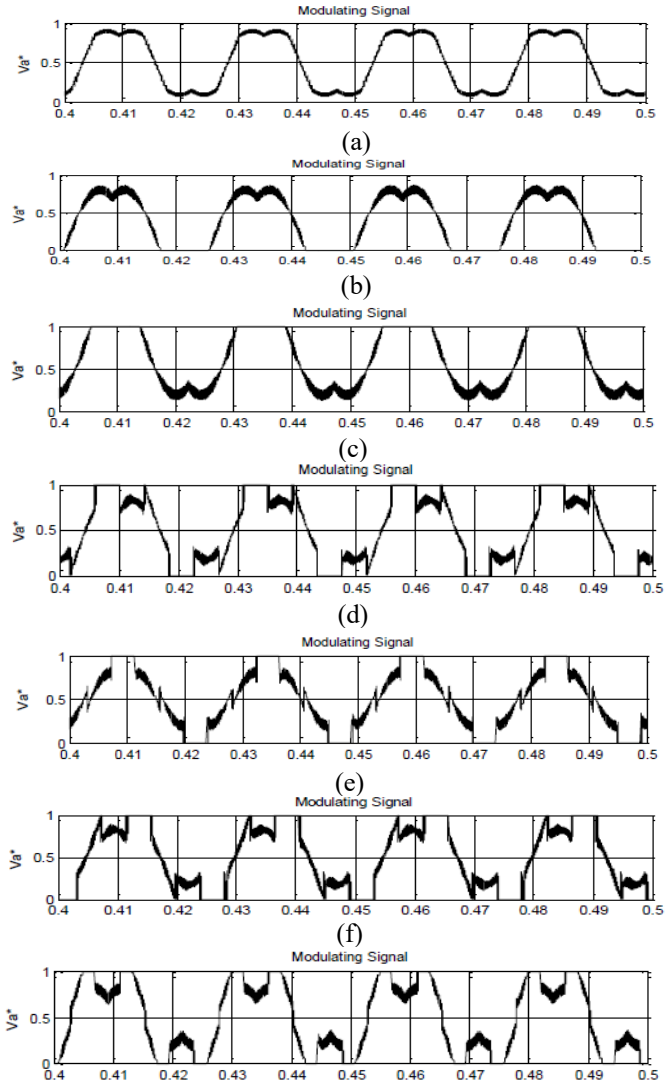

Fig.7. Modulating Waveforms for a) SVPWM, b) DPWMMIN, c) DPWMMAX, d) DPWM0, e) DPWM1, f) DPWM2 and g) DPWM3.

To measure the performance of DTC of OEWIM drive, analysis of phase voltage, stator currents, rotor speed, electromagnetic torque response is mandatory. Therefore let us analyze the above mentioned performance measures for the two PWM schemes. Fig.8 and Fig.9 respectively shows the phase voltage, stator currents, rotor speed, electromagnetic torque response for Decoupled SVPWM and AIS SVPWM based DTC of OEWIM drive operating at 40Hz corresponding to 1200 rpm.

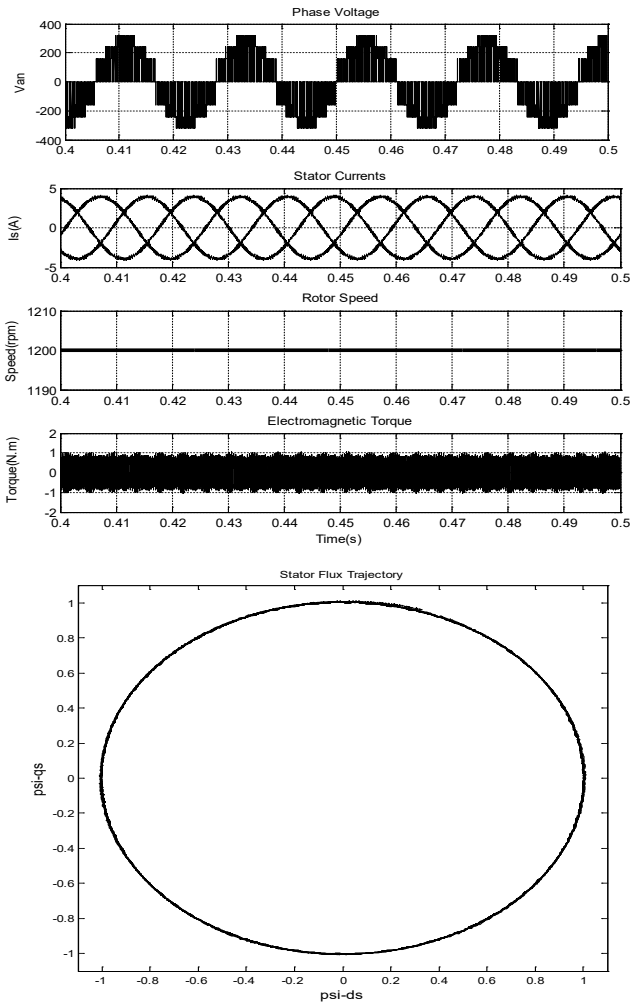

Fig.8. Phase voltage, stator currents, rotor speed, electromagnetic torque and stator flux trajectory of Decoupled SVPWM based DTC of OEWIM.

It is clearly seen that, current drawn by the motor is nearly sinusoidal, stator flux trajectory being unit circle with less ripple (airgap flux is being nearly sinusoidal) and low torque ripple (noiseless operation). Therefore, both Decoupled PWM and AIS PWM schemes exhibit good steady state performance for the DTC of OEWIM drive.

The specifications of the entire drive system were given in Appendix-1. The dc link voltage taken for the drive is 540V. Each of the inverters feeding the dc link voltage of 270V. The total no. of samples per cycle taken for evaluating the losses is 42 for both of the inverters as their dc link voltage is same.

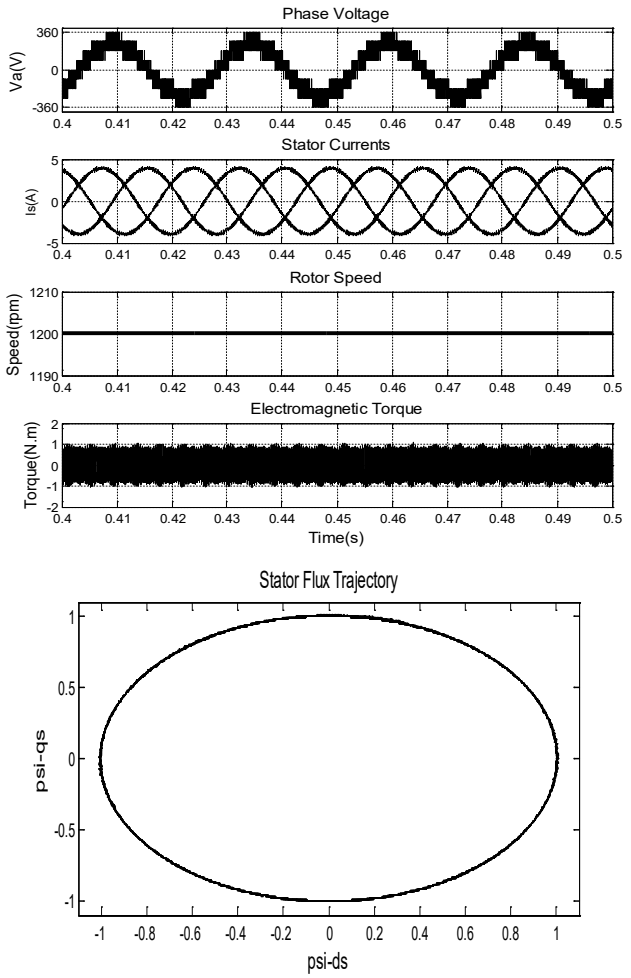

Fig.9. Phase voltage, stator currents, rotor speed, electromagnetic torque and stator flux trajectory of AIS SVPWM based DTC of OEWIM.

Fig.10 and Fig.11 shows the switching loss, conduction loss of the top switch (A1), conduction loss of the top switch (A1) and conduction loss of the bottom diode (D4) respectively for Decoupled SVPWM and AIS SVPWM based drive operating at 40Hz corresponding to 1200 rpm.

The simulation study for the loss calculation of three level inverter fed DTC of OEWIM drive system was carried out by using MATLAB/Simulink. The data required to evaluate the switching and conduction loss is: t_{ri} = 2μs, t_{fi} = 4μs, t_{rv} = 2μs, t_{fv} = 1μs and V_{on}= 1V was taken identical for Decoupled SVPWM and DPWM schemes.

Table 4 and Table 5 shows the switching losses, conduction losses and total dual inverter losses versus modulation index and operating frequency respectively for Decoupled PWM and AIS PWM schemes-based drive.
It is clear that, as the modulation index increases, switching losses and total dual inverter losses increases towards linear modulation index (m=0.866) corresponding to 50Hz frequency. Further increase in modulation index corresponding to over modulation index (m=1), switching losses and total dual inverter losses decreases since drive operates nearly square wave mode, so that inverters clamped to dc bus i.e no switching action taking place at carrier frequency. In most of the PWM schemes conduction loss increases with modulation index as the fundamental component of the current increases with modulation index.

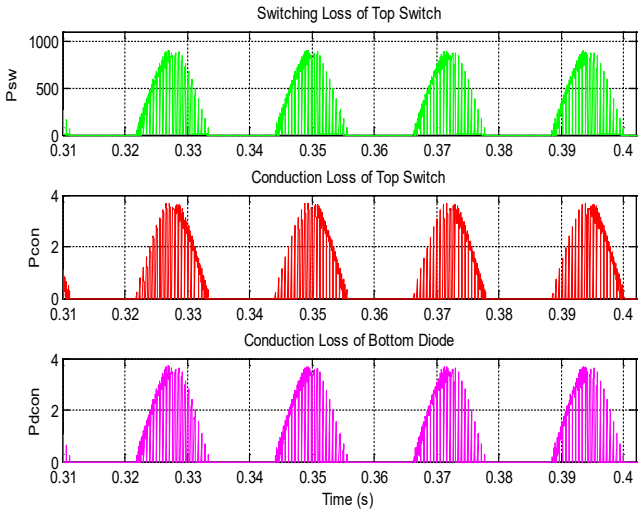

Fig.10. Switching loss of the top switch (A1), conduction loss of the top switch (A1) and conduction loss of the bottom diode (D4) of Decoupled SVPWM for (Ia > 0).

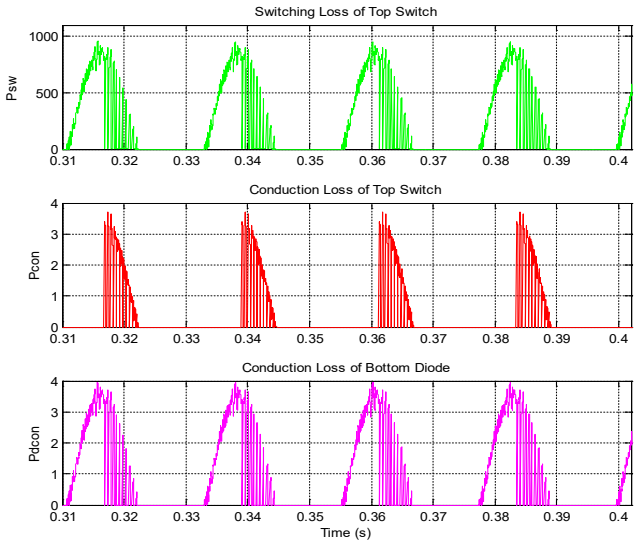

Fig.11. Switching loss of the top switch (A1), conduction loss of the top switch (A1) and conduction loss of the bottom diode (D4) of AIS SVPWM for (I_a > 0).

Fig.12, Fig.14 and Fig.16 shows the Switching losses, conduction losses and total dual inverter losses versus modulation index plot of Decoupled PWM scheme for SVPWM, DPWMMIN, DPWMMAX, DPWM0, DPWM1, DPWM2, DPWM3 techniques.

Fig.13, Fig.15 and Fig.17 shows the Switching losses, conduction losses and total dual inverter losses versus modulation index plot of AIS PWM scheme for SVPWM, DPWMMIN, DPWMMAX, DPWM0, DPWM1, DPWM2, DPWM3 techniques.

Table 4. Switching, Conduction and Total Dual Inverter Losses for Decoupled PWM Schemes

Frequency (Hz)		15	20	25	30	35	40	45	50	57.7
MI (m)		0.259	0.3464	0.433	0.5196	0.6062	0.6928	0.7794	0.866	1
SVPWM	P_{sw}(w)	15.20	36.28	71.16	121.92	194.30	290.82	414.94	506.37	203.70
	P_{con} (w)	4.45	5.95	7.45	8.94	8.76	11.80	11.88	14.55	15.30
	P_{DI} (w)	19.65	42.24	78.61	130.86	203.06	302.61	426.82	520.92	219.00
DPWM MIN	P_{sw}(w)	10.14	24.19	47.44	81.28	129.54	193.88	276.62	325.91	203.70
	P_{con} (w)	1.24	2.22	3.49	5.06	5.61	8.95	11.37	13.96	11.03
	P_{DI} (w)	11.37	26.41	50.93	86.34	135.15	202.83	287.99	339.87	214.73
DPWM MAX	P_{sw}(w)	9.94	23.33	45.75	78.39	124.92	186.95	266.74	348.07	203.70
	P_{con} (w)	7.50	9.46	11.18	12.60	13.64	14.53	15.06	15.20	19.58
	P_{DI} (w)	17.44	32.78	56.93	90.99	138.57	201.48	281.80	363.27	223.28
DPWM0	P_{sw}(w)	10.50	25.05	49.13	84.18	134.16	200.80	284.53	352.94	172.36
	P_{con} (w)	8.75	5.86	7.37	8.81	10.18	11.64	13.14	14.50	13.65
	P_{DI} (w)	19.25	30.91	56.51	92.99	144.35	212.45	297.67	367.44	186.01
DPWM1	P_{sw}(w)	10.50	25.05	49.13	84.18	134.16	200.80	286.50	339.42	203.70
	P_{con} (w)	8.75	5.82	7.27	8.72	10.18	11.65	13.14	14.57	15.37
	P_{DI} (w)	19.25	30.87	56.41	92.90	144.35	212.45	299.64	353.99	219.06
DPWM2	P_{sw}(w)	11.13	25.06	49.13	84.18	134.16	200.80	286.50	352.94	172.36
	P_{con} (w)	8.75	5.81	7.30	8.80	10.25	11.78	13.27	14.56	13.58
	P_{DI} (w)	19.88	30.87	56.43	92.98	144.41	212.58	299.77	367.50	185.94
DPWM3	P_{sw}(w)	10.30	24.19	47.44	81.29	129.55	193.88	276.62	334.55	203.70
	P_{con} (w)	8.75	5.86	7.41	8.93	10.34	11.69	13.28	14.63	15.22
	P_{DI} (w)	19.05	30.05	54.85	90.23	139.90	205.56	289.90	349.19	218.92

Table 5. Switching, Conduction and Total Dual Inverter Losses for AIS PWM Schemes

Frequency (Hz)		15	20	25	30	35	40	45	50	57.7
MI (m)		0.259	0.3464	0.433	0.5196	0.6062	0.6928	0.7794	0.866	1
SVPWM	P_{sw}(w)	7.62	18.14	35.58	60.96	97.15	145.41	207.42	253.18	101.85
	P_{con} (w)	6.53	7.96	7.45	10.95	8.76	13.71	13.23	16.45	17.22
	P_{DI} (w)	14.16	26.19	43.03	71.91	105.91	159.11	220.62	269.58	119.05
DPWM MIN	P_{sw}(w)	5.07	12.09	47.44	40.64	129.54	96.94	138.30	162.95	101.85
	P_{con} (w)	2.33	4.23	3.49	7.11	5.61	10.92	13.47	15.80	13.00
	P_{DI} (w)	7.37	16.32	50.93	47.75	135.15	107.84	151.77	178.75	114.85
DPWM MAX	P_{sw}(w)	4.97	11.66	45.75	39.19	124.92	93.47	133.37	174.03	101.85
	P_{con} (w)	9.42	11.56	11.18	14.54	13.64	16.42	17.15	17.32	21.54
	P_{DI} (w)	14.37	23.16	56.93	53.69	138.57	109.87	150.47	191.33	123.35
DPWM0	P_{sw}(w)	5.25	12.52	49.13	42.09	134.16	100.40	142.22	176.47	86.18
	P_{con} (w)	10.73	7.95	7.37	10.71	10.18	13.53	15.25	16.57	15.57
	P_{DI} (w)	15.95	20.42	56.51	52.79	144.35	113.90	157.42	192.97	101.68
DPWM1	P_{sw}(w)	5.25	12.52	49.13	42.09	134.16	100.40	143.20	169.71	101.85
	P_{con} (w)	10.73	7.81	7.29	10.82	10.18	13.79	15.20	16.41	17.30
	P_{DI} (w)	15.95	20.32	56.41	52.89	144.35	114.00	158.4	186.11	119.15
DPWM2	P_{sw}(w)	5.56	12.53	49.13	42.09	134.16	100.40	143.25	169.71	86.18
	P_{con} (w)	10.73	7.81	7.30	10.82	10.25	13.80	15.10	16.41	15.40
	P_{DI} (w)	16.26	20.34	56.43	52.89	144.41	114.20	158.35	186.12	101.58
DPWM3	P_{sw}(w)	5.15	12.09	47.44	40.64	129.55	96.94	138.31	167.27	101.85
	P_{con} (w)	10.73	7.86	7.41	10.90	10.34	13.79	15.20	16.50	17.20
	P_{DI} (w)	15.85	19.95	51.54	90.23	139.90	110.63	153.51	183.77	119.05

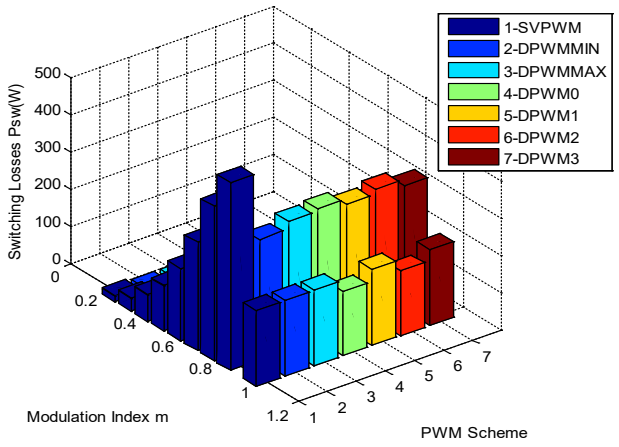

Fig.12. Switching losses versus modulation index plot of Decoupled PWM scheme for SVPWM, DPWMMIN, DPWMMAX, DPWM0, DPWM1, DPWM2, DPWM3.

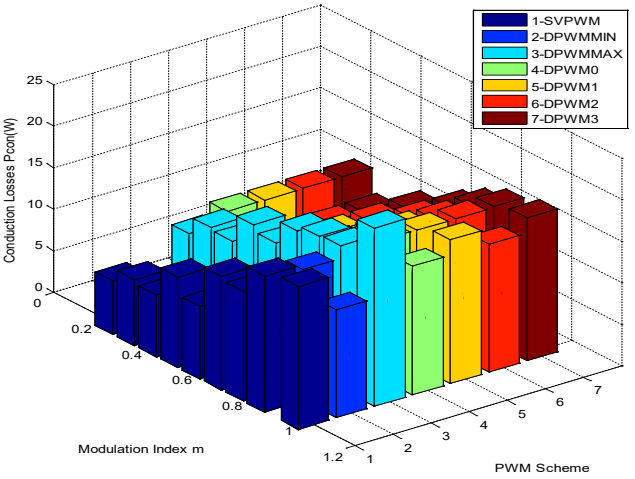

Fig.15. Conduction losses versus modulation index plot of AIS PWM scheme for SVPWM, DPWMMIN, DPWMMAX, DPWM0, DPWM1, DPWM2, DPWM3.

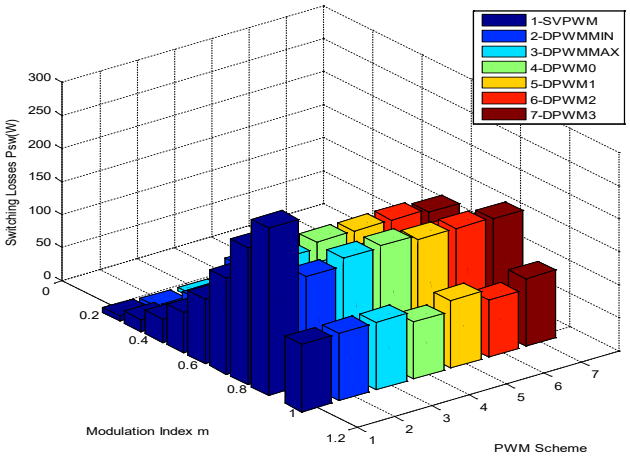

Fig.13. Switching losses versus modulation index plot of AIS PWM scheme for SVPWM, DPWMMIN, DPWMMAX, DPWM0, DPWM1, DPWM2, DPWM3.

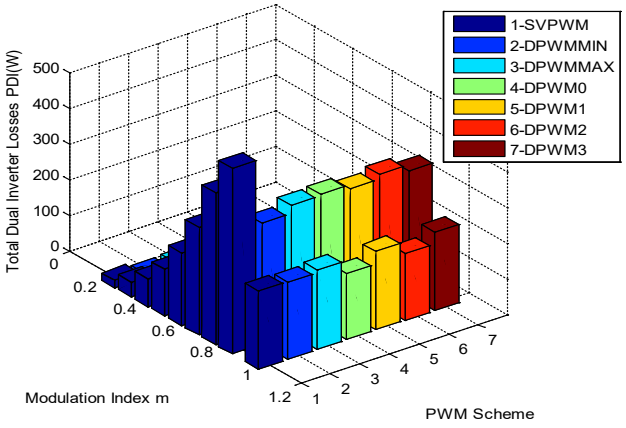

Fig.16. Total Dual inverter losses versus modulation index plot of Decoupled PWM scheme for SVPWM, DPWMMIN, DPWMMAX, DPWM0, DPWM1, DPWM2, DPWM3.

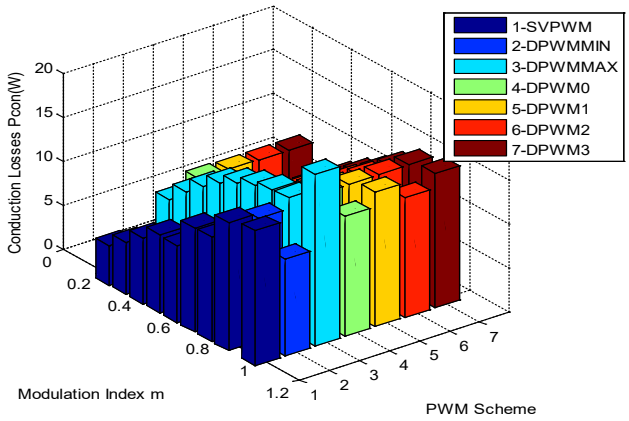

Fig.14. Conduction losses versus modulation index plot of Decoupled PWM scheme for SVPWM, DPWMMIN, DPWMMAX, DPWM0, DPWM1, DPWM2, DPWM3.

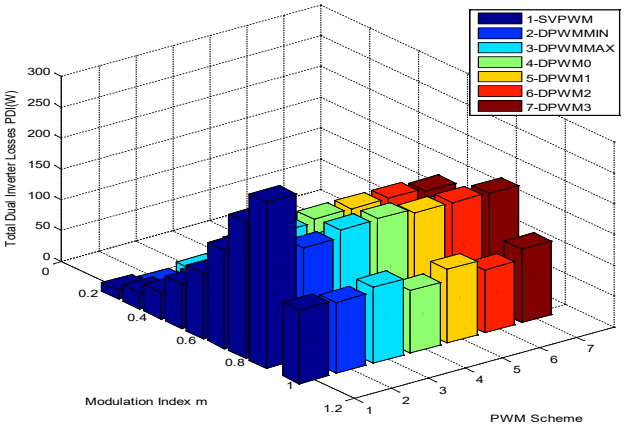

Fig.17. Total dual inverter losses versus modulation index plot of AIS PWM scheme for SVPWM, DPWMMIN, DPWMMAX, DPWM0, DPWM1, DPWM2, DPWM3.

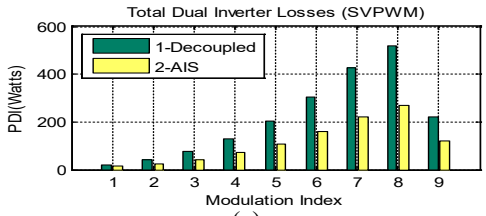

(a)

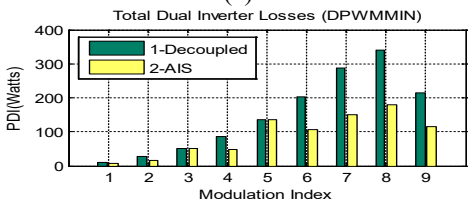

(b)

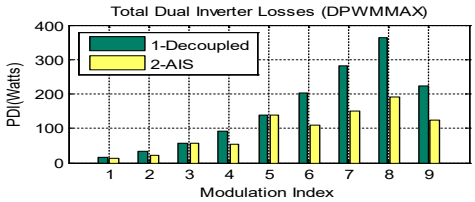

(c)

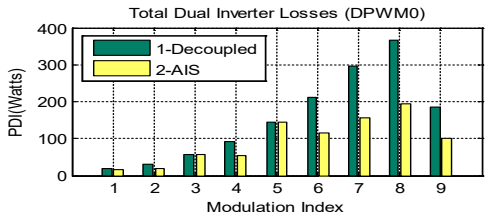

(d)

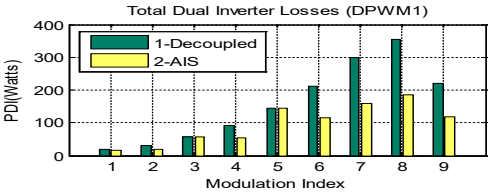

(e)

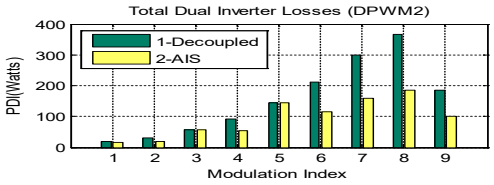

(f)

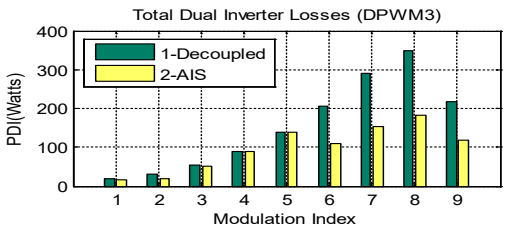

(g)

Fig.18.(a)-18(g) Total dual inverter losses versus modulation index (m1=0.259, m2=0.366, m3=0.433, m4=0.519, m5=0.606, m6=0.692, m7=0.779, m8=0.866 and m9=1.0) plot of Decoupled and AIS PWM schemes for SVPWM, DPWMMIN, DPWMMAX, DPWM0, DPWM1, DPWM2, DPWM3.

7. Experimental Results

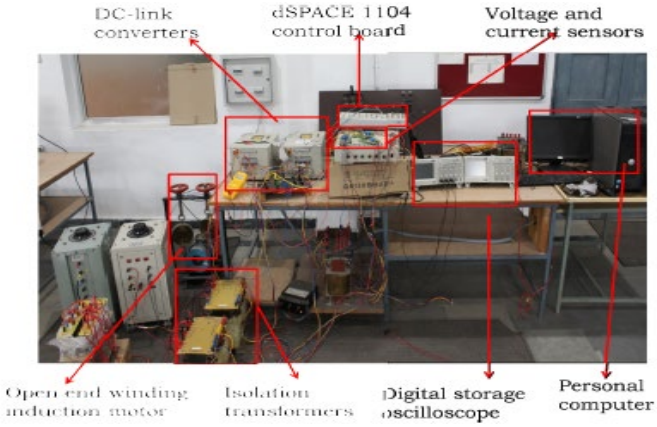

Fig.19. Experimental Bench for the OEWIM Drive.

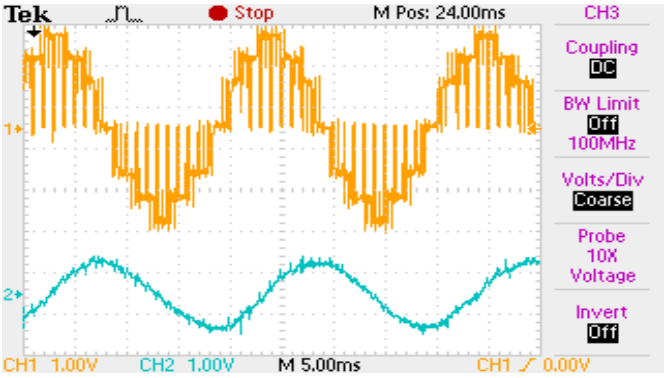

Fig.20. Phase voltage and stator current waveform of the OEWIM drive operating at 1200 rpm corresponding to 40Hz operation for Decoupled SVPWM.

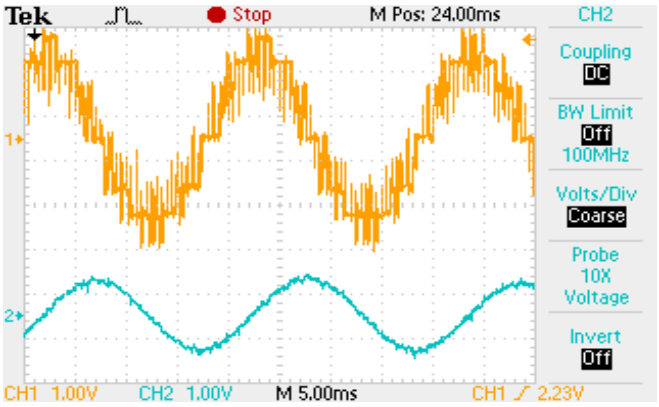

Fig.21. Phase voltage and stator current waveform of the OEWIM drive operating at 1200 rpm corresponding to 40Hz operation for AIS SVPWM.

As seen from Fig.12 and Fig.13, switching losses decreased by about 50% in AIS PWM scheme compared to Decoupled PWM scheme due to clamping action over half of the fundamental cycle, whereas conduction losses (Fig.14 and Fig.15) slightly increased in AIS PWM scheme compared to Decoupled PWM scheme due to clamping action over of the fundamental cycle as well. Total Dual inverter losses (Fig.16 and Fig17) are less in AIS PWM compared to Decoupled PWM for most of the modulation index as shown in Fig.18.

Fig.19 shows the experimental bench for the OEWIM drive. It consists of ac supply feeding two DC link converters, each of which comprises of uncontrolled rectifier at first stage and 9.2 kVA inverter at the second stage, dSPACE 1104 for firing pulse generation and 415V, 50Hz, 1 hp, 1.8A OEWIM. A dc link voltage of 270V is applied to both inverters, hence effective dc link voltage is found to be 540V. A 500 V to 3.3 V regulator (LV20P) is used to measure the phase voltage and LA-55P current sensor is used to measure the current. To observe the voltage and current waveforms Digital Storage Oscilloscope (DSO) was used. For experimental study switching frequency of 1 kHz was employed.

Fig.20 and Fig.21 respectively shows the phase voltage and current waveform of the OEWIM drive operating at 1200 rpm corresponding to 40Hz operation for Decoupled and AIS SVPWM. The phase voltage and current waveforms for DPWM schemes can be obtained in a similar way. In case of Decoupled PWM scheme, both inverters are switching over full cycle, whereas in case of AIS PWM scheme, only one inverter is in switching mode and another inverter is in clamping mode and vice-versa over half cycle and therefore different phase voltage profiles can be obtained as shown in top trace of Fig.20 and Fig.21.

Conclusion

In this paper, the analysis of semiconductor device losses such as switching and conduction losses and total dual inverter losses for DTC of three level dual inverter fed OEWIMD is evaluated with Decoupled SVPWM and DPWM schemes using MATLAB/Simulink. An improvised loss model is used to calculate the losses. In contrary to the conventional loss models, the loss model used in this paper is accurate since anti-parallel diodes and reverse recovery current in them and associated conduction loss are taken into account. Losses calculated from this model are tabulated for various PWM schemes for various modulation indices. Device loss is responsible for junction temperature and associated failure of the device. Hence based on the operating conditions (modulation index), appropriate PWM scheme can be chosen by using the table 4 and table 5.

References

[1] I. Takahashi and T. Noguchi, "A new quick-response and high efficiency control strategy of an induction motor," IEEE Trans. on Ind. Applications, vols. IA-22, pp. 820-827, Sept./Oct. 1986. (Article)

[2] T. G. Habetler F. Profumo M. Pastorelli and L. M. Tolbert, "Direct Torque Control of Induction Machines Using Space Vector Modulation," IEEE Trans. Ind. Appl., vol. 28, no. 5, pp. 1045-1053, Sept./Oct. 1992. (Article)

[3] Y. S. Lai and J. H. Chen, "A new approach to direct torque control of induction motor drives for constant inverter switching frequency and torque ripple reduction," IEEE Trans. Energy Conversion, vol. 16, no. 3, pp. 220-227, Sept. 2001. (Article)

[4] Z. Zhang, Y. Zhao, W. Qiao and liyan Qu, "A Space Vector Modulated Sensorless Direct Torque control for Direct-Drive PMSG Wind Turbines," IEEE Trans. on Ind. Applicat., vol. 50, pp. 2331-2341, Jul./Aug. 2014. (Article)

[5] H. Stemmler and P. Guggenbach, "ConFigurations of high-power voltage source inverter drives," ProC. EPE Conf., Brighton, UK, pp. 7-14, Sept. 1993. (Conference Paper)

[6] K. G. King, “A three phase transistor class-B inverter with sinewave output and high efficiency,” Inst. Elect. Eng. Conf. Pub. 123, 1974, pp. 204–209. (Conference Paper)

[7] M. Depenbrock, “Pulse width control of a 3-phase inverter with nonsinusoidal phase voltages,” Conf. Rec. IEEE Int. Semiconductor Power Conversion Conf., 1977, pp. 399–403. (Conference Paper)

[8] N. Mohan, Undeland and Robbins "Power Electronics: Converters, Applications and Design", Wiley publications, 2003. (Book)

[9] M. C. Di Piazza; M. Pucci, and G. Vitale“ Efficiency modeling in voltage source inverters with several PWM techniques: a unified approach ”, 39th Annual Conference of the IEEE Industrial Electronics Society, IECON, 2013, pp. 700 – 705. (Conference Paper)

[10] S. Srinivas and V. T. Somasekhar “Space-vector-based PWM switching strategies for a three-level dual-inverter-fed open end winding induction motor drive and their comparative evaluation” IET Electr. Power Appl. vol. 2, no. 1, 2008, pp. 19 – 31. (Article)

[11] B. Venugopal Reddy, V. T. Somasekhar, and Y. Kalyan “Decoupled Space-Vector PWM Strategies for a Four-Level Asymmetrical Open-End Winding Induction Motor Drive With Waveform Symmetries” IEEE Trans. Ind. Electron., vol. 58, no. 11, pp. 5130 - 5141, Nov. 2011. (Article).

[12] J. Rodriguez, J. S. Lai, and F. Z. Peng, “Multilevel inverters: A surveyof topologies, controls, and applications,” IEEE Trans. Ind. Electron.,vol. 49, no. 4, pp. 724–738, Aug. 2002. (Article).

[13] L. Suresh, V. K. J. D. Prasad, “Comparative Performance Analysis of Decoupled SVPWM Techniques for a Four Level Open End Winding Induction Motor Drive”, IEEE conf. 2016. (Conference Paper)

[14] W. Jiang, J. Li, J. Wang, J. Wang and X. Huang, “An Overall Minimized Switching Loss Discontinuous PWM Strategy for Neutral Point Clamped Three Level Inverters” IEEE Access, Vol.7,pp. 122387 – 122397, Aug.2019. (Article)

[15] M. Ye , J. Zhang, L. Chen, L. Kang, H. Wu and S. Li, “Modified Modulation Strategy With Balanced Power and Switching Losses Distributed for Seven-Level Cascaded H-Bridge Inverters” IEEE Access, Vol.7, pp.134036 – 134046, Sep.2019. (Article)

[16] H. Peng, Z. Yuan, X. Zhao, B. Narayanasamy, A. Deshpande, A. I. Emon, F. Luo, and C. Chen, "Improved Space Vector Modulation for Neutral-Point Balancing Control in Hybrid-Switch-Based T-Type Neutral-Point-Clamped Inverters with Loss and Common-Mode Voltage Reduction" CPSS Transactions on Power Electronics and Applications, Vol.4,pp.328-338, Dec.2019. (Article)

[17] S. M. Kim, E. J. Lee, J. S. Lee and K. B. Lee, "An Improved Phase-Shifted DPWM Method for Reducing Switching Loss and Thermal Balancing in Cascaded H-Bridge Multilevel Inverter", IEEE Access, Journal Article, Vol.8, pp.187072-187083, Oct 2020. (Article)

[18] S. Bhattacharya, "Three-Level Discontinuous PWM for Loss and Thermal Redistribution of T-NPC Inverter at Low Modulation Index" IEEE Journal of Emerging and Selected Topics in Industrial Electronics, Vol. 1, No. 2, pp.143-151, Oct. 2020. (Article)

[19] Z. Wang, X. Li, X. Xing, B. Duan and C. Zhang, "Simultaneous Switching Loss Reduction and Neutral-Point Voltage Balance Scheme for Single-Phase Three-Level T-Type Inverter", IEEE Transactions on Industry Applications, Vol. 56, No. 6, pp. 6687-6700, Nov/Dec 2020. (Article)

[20] M. R. Chowdhury, M. A. Rahman, M.R. Islam and A. M. Mahfuz-Ur-Rahman, "A New Modulation Technique to Improve the Power Loss Division Performance of the Multilevel Inverters" IEEE Trans. on Industrial Electronics, Vol. 68, No.8,pp.6828-6839, Aug. 2021 (Article)

[21] W. Jiang, H. Jiang, S. Liu, S. Ji and J. Wang, "A Carrier-Based Discontinuous PWM Strategy for T-Type Three-Level Converter With Reduced Common Mode Voltage, Switching Loss, and Neutral Point Voltage Control" IEEE Trans. on Power Electronics, Vol. 37, No.2, pp.1761-1771, Oct. 2021. (Article)

[22] H. Benbouhenni, "Stator Current and Rotor Flux Ripples Reduction of DTC DFIG Drive Using FSTSMC Algorithm" International Journal of Smart Grid, Vol.3, No.4, pp.226-234, Dec.2019 (Article)

[23] Y. Huang, Y. Xu, W. Zhang and J.Zou, "Modified Single-Edge SVPWM Technique to Reduce the Switching Losses and Increase PWM Harmonics Frequency for Three-Phase VSIs" IEEE Transactions on Power Electronics, Vol.35, No.10, pp.10643-10653, Oct. 2020. (Article)

[24] C. Xu and S. Lu, "Practical Online Modulation Method for Current Ripple and Switching Losses Reduction in the Three-Phase Voltage Source Inverters" IEEE Trans. on Power Electronics, Vol. 36, No. 2, pp. 1475-1490 Feb. 2021 (Article)

[25] S. M. Suhel and R. Maurya, "A New Switching Sequences of SVPWM for Six-Phase Induction Motor with Features of Reduced Switching Losses" CES Trans. on Electrical Machines and Systems, Vol. 5, No. 2, pp.100-107, June 2021. (Article)

[26] S. Y. Kim, S. G. Song and S. J. Park, "Minimum Loss Discontinuous Pulse-Width Modulation Per Phase Method for Three-Phase Four-Leg Inverter", IEEE Access, Journal Article, Vol.8, pp.122923-122936, Jul.2020. (Article)

[27] N. K. Bajjuri and A. K. Jain, "Minimization of Current Ripple and Switching Losses in Double Inverter Fed Wound Rotor Induction Machine Drive Using PWM Techniques", IEEE Transactions on Industrial Electronics, Vol. 67, No.5, pp. 3484-3495, May 2020. (Article)

[28] A. R. Teja, S. Figarado and N. Harischandrappa, "Dodecagonal Voltage Space Vector Based PWM Techniques for Switching Loss Reduction in a Dual Inverter Fed Induction Motor Drive" IEEE Journal of Emerging and Selected Topics in Industrial Electronics, Vol.1, No.2, pp.182-191, Oct. 2020 (Article)

[29] C. Ibtissam, E. M. Berkouk, J. P. Gaubert, M. Kermadi, N. Sabeur and S. Mekhilef, "An Improved Discontinuous Space Vector Modulation for Z-Source Inverter with Reduced Power Losses", IEEE Journal of Emerging and Selected Topics in Power Electronics, Vol. 9, No. 3, pp.3479-3488, June 2021. (Article)

Appendix-1

Ratings of the Induction Motor:

V = 400 Volts, P = 4 kW, p = 4, N_{rated} = 1470 rpm, f =50 Hz and T_{rated} =30 N-m.

Parameters of the Induction Motor:

R_s = 1.57 Ω, R_r = 1.21 Ω, L_m = 0.165 H, L_s = 0.17 H, L_r = 0.17 H and J = 0.089 Kg - m^2